

Accepted Manuscript

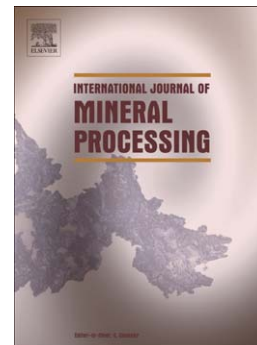
A semi-mechanistic model of hydrocyclones – developed from industrial data and inputs from CFD

M. Narasimha, A.N. Mainza, P.N. Holtham, M.S. Powell, M.S. Brennan

PII: S0301-7516(14)00105-7
DOI: doi: [10.1016/j.minpro.2014.08.006](https://doi.org/10.1016/j.minpro.2014.08.006)
Reference: MINPRO 2641

To appear in: *International Journal of Mineral Processing*

Received date: 22 August 2013
Revised date: 6 June 2014
Accepted date: 16 August 2014



Please cite this article as: Narasimha, M., Mainza, A.N., Holtham, P.N., Powell, M.S., Brennan, M.S., A semi-mechanistic model of hydrocyclones – developed from industrial data and inputs from CFD, *International Journal of Mineral Processing* (2014), doi: [10.1016/j.minpro.2014.08.006](https://doi.org/10.1016/j.minpro.2014.08.006)

This is a PDF file of an unedited manuscript that has been accepted for publication. As a service to our customers we are providing this early version of the manuscript. The manuscript will undergo copyediting, typesetting, and review of the resulting proof before it is published in its final form. Please note that during the production process errors may be discovered which could affect the content, and all legal disclaimers that apply to the journal pertain.

A SEMI-MECHANISTIC MODEL OF HYDROCYCLONES – DEVELOPED FROM INDUSTRIAL DATA AND INPUTS FROM CFD

M. Narasimha^{a*}, A.N. Mainza^b, P.N. Holtham^c, M.S. Powell^c, M. S. Brennan^c

^a Department of Chemical Engineering, IIT Hyderabad, Ordinance Factory Estate, Yeddumailaram, 502205, India.

^b Centre for Minerals Research, Chemical Engineering, University of Cape Town, Rondebosch, 7701, Cape Town, South Africa

^c JKMRC, Sustainable Mineral Institute, The University of Queensland, Isles Road, Indooroopilly 4068, Queensland, Australia.

ABSTRACT

The flow behavior in hydrocyclones is extremely complex, leading the designers to rely on empirical equations for predicting cyclone performance. A number of classifying cyclone models have been developed and used in mineral comminution circuit simulators in the past. The problem with these empirical cyclone models is that they cannot be used outside the range of conditions under which they were developed. A semi-mechanistic hydrocyclone model is developed using the dimensionless approach based on both the fluid mechanics concepts from Computational fluid dynamics (CFD) simulations and the wide range of industrial cyclone performance data. The improved model consist a set of equations for the water split to underflow (R_f), reduced cut-size (d_{50c}), throughput (Q) and sharpness of the separation (α). The model for R_f , d_{50c} , Q gives a very good fit to the data. The alpha model shows reasonable correlation for the cyclone design and operating conditions. Additional data sets were used to validate the new hydrocyclone model by comparing the predictions of the model equations with the experimental results.

Key words: Hydrocyclone, mathematical modelling, computational fluid dynamics, classification

* Corresponding author: narasimha@iith.ac.in, Fax: +91 40 2301 6003

1. Introduction

Feed slurry is introduced under the high pressure tangentially into the hydrocyclone. This creates the centrifugal force and the flux of particles toward the radial positions, thus leading to phase separation. Although the design and operation of the hydrocyclone is simple, the flow behavior is complex. This poses a challenge when developing a mathematical model that can be applied for the design and the optimization of this device. As a result many designers rely on empirical equations for predicting cyclone performance. In addition to capacity, hydrocyclones are usually modelled in terms of partition curve properties namely; cut-size, flow split and sharpness of separation. One of the first comprehensive model that was used to predict the performance of industrial hydrocyclones was developed by Lynch and co-workers at University of Queensland (Lynch and Rao, 1968; Rao, 1966). This model was applied to predict the cyclones performance at Mount Isa Mines, Australia. The methodology has been successfully adopted in the minerals industry (Lynch, 1977). The relationships in their model were derived from analysis of experimental data collected from numerous trials performed to capture the effect of operational and geometric variables. A number of classifying cyclone models, with some mechanistic basis, has been developed over the past four decades (Nageswararao, 1978; Plitt, 1976; Svarovsky, 1984). The two commonly used in simulation packages are Plitt (1976) and Nageswararao (1978) which have been incorporated into the MODSIM and JKSimMet software respectively. These models have been successfully used in grinding circuit simulations.

The Plitt (1976) model consist equations for cyclone throughput, volumetric flow split, cut-size and sharpness of classification using the original data from Rao's (1966) tests on a 50.8-cm diameter hydrocyclone along with those from 3.1, 6.2 and 15.2 cm diameter units. This model implicitly assumes that the cyclone performance is independent of feed material characteristics and is claim that performance could be estimated with reasonable accuracy even when no experimental data are available.

The Nageswararao (1978) model consists of three basic equations: The capacity equation relating feed flow rate with operating pressure, and two partition curve properties namely; the water recovery to the underflow (R_f) and the corrected cut-point, (d_{50c}). The Whiten equation (Lynch and Rao, 1975) is then used to estimate the sharpness of separation (α). These three equations include the material-specific parameters that take up the effects of differences in feed size distribution solids content and the influences of cyclone geometry variables.

Other hydrocyclone models include (Asomah, 1996; Castro, 1990; Kojovic, 1988; Lynch et al., 1975; Marlow, 1973; Tavares et al., 2002; Xiao, 1997). Asomah (1996) included the cyclone inclination to the vertical position and attempted to develop an explicitly equation for the sharpness of separation. Castro (1990) re-fitted a number of additional data sets to obtain slightly different values of the exponents in the Nageswararao (1978) equations. Combining the first industrial database on cyclones generated at JKMRRC (Rao, 1966) with the laboratory data (Plitt, 1976) developed an alternative general-purpose cyclone model.

The problem with the above-mentioned empirical cyclone models is that they cannot be used outside the range of conditions under which they were developed. Furthermore, any change to the design of the cyclone (e.g. cone angle, body length etc) means that the empirical constants have to be refitted.

In view of this shortcoming, inputs from mathematical models based on fluid mechanics are highly desirable. Alternatively multi-phase flow in cyclones can be modelled more fundamentally by Computational Fluid Dynamics (CFD). CFD provides a means of predicting velocity profiles under a wide range of design and operating conditions.

There are numerous numerical studies on the flow and the particle motion in hydrocyclones (Boysan et al., 1982; Brennan et al., 2007; Delgadillo and Rajamani, 2005; 1996; He et al., 1999; Hsieh and Rajamani, 1988; Hsieh and Rajamani, 1991; Narasimha et al., 2006a; Narasimha et al., 2007; Narasimha et al., 2005; Nowakowski et al., 2004; Nowakowski et al., 2000; Suasnabar, 2000 and Narasimha 2010) and these studies have used a wide range of turbulence and multiphase models. It is well understood that in future studies, the focus should be to model the three-dimensional flow in a hydrocyclone with at least the Reynolds stress model/LES. The particle simulations should at least include the effects of the turbulence on the particles. All these developed models are mainly applicable to low to moderate feed solid concentration levels. A successful CFD model would be a useful tool for studying design dimensions. More importantly, alternative geometries may be rapidly examined. However, CFD simulations can be used to provide information on key variables that affect the performance of the hydrocyclone alone and how they can be presented in terms of dimensionless terms that can be incorporated in semi-empirical models.

In this paper, the development of improved semi-empirical hydrocyclone model is attempted by collecting an extensive historical data base. Inputs on particle classification mechanism elucidate from CFD were used to understand and identify the key flow variables that affect the cyclone performance when classifying the particles by size wise. Although historical data covered a wide range of conditions further tests were performed at both full scale and pilot-plant to fill the gaps, especially at low to moderate feed solids concentration and for different cone sections. A new cyclone model structure based on a dimensionless approach that incorporates the variables suggested to be important from the CFD is reported and model validation results are given.

2. Data Collection

A large number of data sets containing the performance of hydrocyclones when operated under different conditions and various designs was compiled and used for the development of the model. The composition of the data includes larger portion of the historical data, the data collected from series of tests conducted with pilot and laboratory size cyclones to fill the gaps in the database such as hydrocyclones operating at on low feed solids and the data from hydrocyclones fitted with various cone angles.

2.1. Historical data

The following is a summary of researchers who have extensively measured the hydrocyclone performance data used for the development of the new model reported in this work.

- (Rao, 1966)
- (Nageswararao, 1978)
- (Castro, 1990)
- (Asomah, 1996)
- (Hinde et al., 1979)

Rao (1966) conducted closely controlled tests with 150, 250, 381, and 508 mm size Krebs cyclones, using limestone and copper ore slurries. The aim of the work was to study the effects of change in the cyclone outlets (vortex finder and spigot) dimensions, the feed pressure and the concentration of solids in the feed pulp on the capacities and classification performance. Lynch et al. (1975) developed the linear cyclone models using these data sets.

Nageswararao (1978) conducted classification tests on 100, 150, 250 and 381 mm size Krebs cyclones by varying the design and operating conditions and obtained a wide range of data with limestone as a feed material. Further the influence of cone angle and cyclone length was studied using a 150 mm Krebs cyclone. Nageswararao (1978) had developed an industrial classifying cyclone model using the Lynch and Rao (1975), Rao (1966) and the above mentioned data sets. This model has been widely used in mineral comminution circuit simulator, JKSimMet.

Hinde et al., (1979), Mackay et al., (1981) performed tests using a large diameter industrial cyclone (31 inch cyclone) with a tangential inlet and the feed material for the test work comprised heavy minerals. The aim of the test work was to evaluate the influence of the spigot size, inlet diameter, feed flow rate and feed solids concentrations on the classifying performance of the hydrocyclone.

Castro (1990) conducted experiments in a 10 inch Krebs cyclone to determine the effect of rheology on the hydrocyclone performance. These tests had two levels (fine and coarse) feed size distribution with three levels of fluid viscosities. The feed solids concentration was varied from 25 wt% to 75 wt%. Further the industrial tests were also conducted to validate the developed model in a 508 mm Krebs cyclone operating with Mount Isa Copper ore, Australia. This series of tests treated the slurry using different vortex finder and spigot diameters and used two levels of feed solids concentration.

Asomah (1996) conducted an extensive series of experiments in 4 and 20 inch cyclones while studying the effect of inclination on cyclone performance. For the first time a cyclone model for the inclination effect was built and validated with limited data. In addition to the above data bases, a number of datasets on 15, 10 and 6 inch Warman cyclones were provided by JKTech to supplement the historical data. These data sets were used for validating the new cyclone model.

A review of the historical database indicated a number of gaps such as:

- Most of the previous historical data has feed solids concentration in range of 40-70 wt%. Feed solids data below 40wt% is essential for developing a generalized hydrocyclone model.
- Some of the historical data sets from Lynch and Rao (1975) test work didn't include large scale cyclones tests.

- The historical data has a limited range of data on cone angle affect.
- Limited range of data for large diameter cyclones below 40 wt% feed solid concentration.

Additional experiments were performed covering the conditions that were missing in the database compiled from historical data. The additional experiments performed included:

2.2. Experimental work at JK pilot plant

Work was conducted using a 10 inch Krebs cyclone in the JKMRC pilot plant. Thirty two tests were conducted using the two cone angle conical sections; 10.5 and 20 degrees, and feed solids concentrations in the range of 10-30 % solids by mass of limestone. Spigot diameter and feed pressure were also varied.

2.3. Low feed solids test work performed at Krebs Engineers, US

37 tests on a 20 inch cyclone were conducted by Mainza et al., (2006) at Krebs Engineers in Tucson has been included in the model data sets. The design of the cyclone test rig was based on the rig designed for testing the three product cyclone at Eastern Platinum, Lonmin (Mainza, 2006). The provision to measure the feed and product flow rates at the Krebs Engineers cyclone testing facility made it possible to perform tests with a bigger diameter cyclone and the rig enabled accurate measurements of the flow split which are difficult to obtain in cyclones of this size.

For the tests by Mainza et al., (2006) the feed % solids, spigot diameter, and feed inlet pressure were varied. (Mainza et al., 2006) conducted 26 tests on a conventional cyclone with just a gMax inlet and 11 tests on a complete gMax design. gMax design is one of the latest Krebs's design with multi-cone sections and an improved inlet design.

Table 1: Data collection

2.4. Data compilation

A summary of the data used for model development is given in Table 1. The data were collected from 4, 6, 10, 15, 20, and 30 inch hydrocyclones operating with various minerals are collated for

model development. A total of 479 hydrocyclone tests has been collected and compiled (Table 1) into a data set for model development and validation.

2.5. Quality of the data

The efficiency curves for 479 data sets have been plotted to check the data quality. It has been found that most of the data sets appear to be good as far as the efficiency curve is concerned, but only a few data sets have obvious measurement errors. Some data sets appeared have poor efficiency curves for modeling studies. Figure 1 shows an example of efficiency curves from the high quality data used in the model. Apart from the standard efficiency curve anomalies, a further check on the quality of data was made using the standard deviations on the parameter estimates of each and every efficiency curve used. For example, as a result of the sampling problems and size measurement handling errors encountered in the work of Mainza et al., (2006) the standard deviations of the efficiency curve fitting parameters listed in Table 2 were high. It should also be mentioned that the highest inconsistency were noted at alpha values of approximately 4.0. In instances where the average standard deviation level was high a decision was made to exclude the data from further analysis. The e results from the example being considered show a significant problem with the parameter estimation for part of the model building data, as shown in Figure 1

Figure 1: Cyclone efficiency curves for Krebs 20 inch design

3. CFD inputs for model development

As reported elsewhere by authors (Narasimha, 2010), the hydrocyclones can be modelled successfully by multi-phase CFD model up to moderate solids concentrations. The information from the CFD simulations presented in this work was incorporated in the semi-empirical model developed in this work.

3.1. Tangential velocity

In a hydrocyclone, the tangential velocity is the key velocity component in separating the particle in a centrifugal field. The tangential velocity of the fluid in a given cyclone increases as radius

decreases from the cyclone wall and reaches a maximum and then decreases as the air-core is approached. The free vortex condition where there is complete conservation of angular momentum is thus being approached. Bradley (1965) outlines the tangential velocity definition in the outer regions of a free vortex by the following tangential velocity relationship for any given hydrocyclone design and operating conditions.

$$V = 4.5 \left(\frac{D_i}{D_c} \right)^{1.13} V_i \left(\frac{R_c}{R} \right)^n \quad (1)$$

Where V is the tangential velocity component, D_i is the equivalent inlet diameter, D_c is the diameter of the cyclone, V_i is the inlet velocity, R_c is cyclone radius, R is the radial position and n is constant.

Further the tangential velocity of the fluid near the wall of cyclone can be deduced as

$$V_t = 4.5 \left(\frac{D_i}{D_c} \right)^{1.13} V_i \quad (2)$$

The parameter n was estimated from the CFD two-phase simulations performed on various cyclones which were conducted in FLUENT using the procedure outlined in the CFD approach reported elsewhere (Narasimha, 2010). Figure 2 & 3 show the predicted CFD tangential velocity profiles at different elevations were extracted and fitted with the empirical equation (1) in a D6, D10 and D15 Krebs designs. It was found that the smaller cyclone (D6) had a lower value for n parameter compared to that of a large diameter cyclone (D15). It was also found that the peripheral velocity near the wall can be estimated using Equation (2). Equation (2) is used in the model development as a key variable instead of the inlet pressure, which was used in all previous cyclone models.

Figure 2: Comparison of tangential velocity profiles with $n=0.71$ in D6 cyclone

Figure 3: Comparison of tangential velocity profiles with (a) $n=0.76$ in D10 cyclone and (b) $n=0.77$ in D15 cyclone

3.2. Turbulent diffusion coefficient

The multi-phase turbulence analysis discussed by authors (Narasimha, 2010; Narasimha et al., 2010) shows that turbulent mixing becomes less important with larger particles but has a significant influence on the dispersion of fine particles.

Further an attempt was made to test and use a simple empirical correlation for diffusion coefficient calculations available in the literature for hydrocyclones. To this end, a number of equations were tested and analysed (Narasimha et al., 2010). It was observed that equation (3) developed by (Neesse, 1971) for calculating the diffusion coefficient in hydrocyclones is suitable since it is directly related to the hydrocyclone geometry, specifically to the cone angle.

$$D_t = k * D_c * \tan(\theta/2) \quad (3)$$

Where θ is the cone angle, k is the radial velocity constant.

Usually the variation in cone angle changes the flow reversals and the locus of zero vertical velocity (LZVV) near the bottom of the conical section of hydrocyclones. He and Laskowski, (1994), Mangadoddy Narasimha et al., (2007), Narasimha et al., (2007) showed that the flow reversals are responsible for an increased dispersion of particles in the conical section. Hence equation (3) based on Neesse, (1971) was adopted for the model development reported in this work.

3.3. Slurry viscosity

It is important to consider slurry rheology to understand the separation mechanism for hydrocyclones (He and Laskowski, 1994; Narasimha, 2007; Shi, 1994). It was shown by many researchers that the viscosity of a suspension increases with solids concentration. Typical rheograms for magnetite (He and Laskowski, 1994) and silica (Mangesana, 2008) which display non-Newtonian behaviour are shown in the Figure 4 and 5. From Figure 4, it was observed that though the overall flow curve shows a non-Newtonian behaviour, with shear thinning as shear rate increases, the apparent viscosity (slope of the rheogram) is constant at higher shear rates

(>200). This means at high shear rates, the slurry behaviour can be approximated like to a Newtonian fluid, though dependent on local solids concentration.

Figure 4: Rheograms of magnetite slurry (He and Laskowski, 1994)

Figure 5: Rheograms of silica slurry (Mangesana, 2008)

Based on CFD studies conducted in dense medium cyclones & hydrocyclones by the authors (Narasimha, 2010; Narasimha et al., 2006b), it was observed that the shear rate inside the cyclone is usually $>100 \text{ s}^{-1}$ except near the air-core and wall regions. Therefore using the shear independent viscosity model as an approximation was found to be good enough to describe the flow resistance in cyclones.

A model that describes viscosity as a function of solids concentration was initially considered for the development of a semi-mechanistic cyclone model as an independent variable. This was defined as given in equation (4) (Ishii and Mishima, 1984). A dimensionless form (μ_m/μ_w) was used. Where μ_m and μ_w are slurry and water viscosities respectively.

$$\mu_m = \mu_w * \left(1 - \frac{fv}{0.62}\right)^{-1.55} \quad (4)$$

Though the Equation (4) was meant to apply for cases involving solids in the liquid system, it does not take into account any fine fraction on viscosity of slurries and it assumes a Newtonian behaviour for all shear rates for a given system.

Figure 6: Comparison of predicted slurry viscosity by (Ishii and Mishima, 1984) and new model with the measured values

The additional effect of the fine fraction below 38 μm is assumed to have an independent effect on viscosity and is calibrated against the available measured viscosity data (Asomah, 1996; Castro, 1990). The prediction capability of equation (4) and (5) were compared by testing them using the experimental data from cyclones operated at different conditions. The predicted relative viscosity by equation (5) was found to be reasonably close to the observed values compared to those predicted by equation (4) as shown in Figure 6. The standard error associated with equation (5) predictions was about 23%. The final modified viscosity model is shown in equation 5.

$$\frac{\mu_m}{\mu_w} = \left(1 - \frac{f_v}{0.62}\right)^{-1.55} (F_{-38\mu})^{0.39} \quad (5)$$

3.4. Hindered settling

Apart from influencing slurry viscosity, the feed solids concentration also changes the settling rate of particle in liquid-solid systems. Nageswararao (1978) cyclone model used λ ($\lambda = f_v / (1 - f_v)^3$) as the indication of feed solids effect on settling rate of particles. This has been derived from Steinour (1944) hindered settling model given in Equation (6) for specific cases where the feed solids fraction (f_v) is more than 0.3.

$$\frac{V_h}{V_t} = \frac{(1 - f_v)^2}{10^{(1.82 * f_v)}} \quad (6)$$

Where f_v is the volumetric fraction of solids in the pulp.

V_H is the hindered settling maximum velocity

V_t is the maximum velocity of the particle under free settling conditions.

Equation (6) was found to describe the hindered settling effect well suited from dilute slurries to dense slurries (Steinour, 1944). The multi-phase CFD simulations described by Narasimha, (2010) also emphasizes the importance of correcting the drag law based on the (Richardson and Zaki, 1954) hindered settling equation to improve the predictability of particle classification.

4. Semi-mechanistic model

The development of an improved hydrocyclone model is attempted by collecting an extensive data base as described in the data collection section. Inputs from Computational Fluid Dynamics (CFD) on particle classification mechanism from were considered to understand and identify the key flow parameters that affect the cyclone performance while separating the particles by size basis. Using the experimental data and inputs from CFD a new cyclone model structure based on the dimensionless approach was then formulated.

The most commonly changed variables for cyclones in industrial practice are Du , Do , P or Q_f, f_s or ρ_p, μ_m , and θ . However the influence of the inlet diameter (D_i), cone angle (θ) and cyclone length (L_c) on hydrocyclone performance are also important and therefore need to be known when selecting the optimum design for any specific duty. Therefore in developing the hydrocyclone model for the present work, the following variables were considered: D_c, D_o, D_u, D_i, P or Q_f, f_s or $\rho_p, \mu_m, \rho, i, L_c, f_v, g$. These are the same variables used by (Nageswararao, 1978) except the inclination angle (i).

A number of additional compound dimensionless groups like Reynolds number, G-forces, viscosity ratio, turbulent diffusion coefficient (related to the flow reversals in the cyclone) are defined in order to develop various cyclone model structures to predict the accurate values of R_f, d_{50c}, α, Q . The definitions of these groups are discussed in the following section.

4.1. Reynolds Number

The conditions of flow in cyclone in general can be expressed in terms of Reynolds number R_e . The definition is generally chosen in terms of cyclone diameter and feed inlet velocity, that is:

$$R_e = \frac{uD_c\rho}{\mu} \quad (7)$$

Where $u = v_i = \frac{Q_f}{\frac{\pi}{4}(D_i^2)}$

Whenever R_e used for any model equations, the independent effect of viscosity was not included separately.

4.2. Centrifugal force

The major driving force for the separation of solids particles in a hydrocyclone is the centrifugal force generated by the rotational flow of slurry. In general, the higher the centrifugal force the less underflow water split (R_f) and the higher separation efficiency. To some extent, R_f and d_{50C} depends on G forces around the spigot area. Instead of P or Q_f variables, a new compound term called the G-number, which is the ratio of centrifugal forces at the wall of the cyclone to gravity forces was used in the model development. This was defined as shown in equation (8).

$$\text{G-number} = \left(\frac{V_t^2}{R_{\max} g} \right) \quad (8)$$

Where V_t is the tangential velocity as has been calculated using equation (2) as suggested by Lilge (1962) and Tavares et al., (2002)

4.3. Turbulence diffusion co-efficient

To some extent, the turbulence dispersion of fine particles also causes the entrainment between the coarser particles and flow along with water to underflow. In order to account for these effects on R_f , d_{50C} and alpha a simple normalized turbulence diffusion coefficient shown in equation (3) suggested by Neesse (1971), Neesse et al., (1986) was used.

$$\frac{D_t}{k D_c} = \text{Tan}(\theta/2) \quad (9)$$

Where θ is the cone angle, k is the radial velocity constant, D_t is turbulent diffusion coefficient and D_c is the cyclone diameter.

4.4. Hydrocyclone model equations

A generalised model for industrial hydrocyclones, which includes equations for water split to the underflow (R_f), corrected cut size (d_{50c}), sharpness of separation (α), and capacity (Q) was

formulated to evaluate their performance. The following dimensionless variables were used in the model:

- reduced vortex finder, D_o/D_c
- reduced spigot, D_u/D_c
- reduced inlet, D_i/D_c
- reduced length of the cylindrical section, L_c/D_c
- Normalized turbulent dispersion coefficient (cone angle), $D_t/(kD_c) = \tan(\theta/2)$

The diameter of the cyclone D_c was chosen as the characteristic dimension of length to which all other physical cyclone dimensions were normalized.

The operating variables consider were

- the relative slurry viscosity, $\frac{\mu_m}{\mu_w}$
- the hindered settling factor, $\frac{V_h}{V_t} = \frac{(1-f_v)^2}{10^{(1.82*f_v)}}$
- G-forces, $\left(\frac{V_t^2}{R_{\max} g}\right)$ or Reynolds number, Re
- relative particle density, $\frac{\rho_s - \rho_f}{\rho_f}$ or $\frac{\rho_s - \rho_f}{\rho_s}$

Taking into account all the practical hydrocyclone models developed by other researchers, together with the current state-of-art models and latest test results, the following equations, were investigated:

The d_{50c} equation

$$\frac{d_{50c}}{D_c} = f_d \left(\frac{D_o}{D_c}, \frac{D_u}{D_c}, \text{Re}, \frac{V_h}{V_t}, \frac{\rho_s - \rho_f}{\rho_f}, \frac{1}{\tan(\theta/2)}, \frac{L_c}{D_c}, \frac{D_i}{D_c}, \text{Cos}\left(\frac{i}{2}\right) \right) \quad (10)$$

The water split equation

$$R_f = f_w \left(\frac{D_o}{D_c}, \frac{D_u}{D_c}, \frac{v_t^2}{R_{\max} g}, \frac{V_h}{V_t}, \frac{\rho_s - \rho_f}{\rho_f}, \frac{\mu_m}{\mu_w}, \frac{1}{\tan(\theta/2)}, \frac{L_c}{D_c}, \cos(i/2) \right) \quad (11)$$

The alpha equation

$$\alpha = f_\alpha \left(\frac{D_o}{D_c}, \frac{D_u}{D_c}, \frac{v_t^2}{R_{\max} g}, \frac{V_h}{V_t}, \frac{\rho_s - \rho_f}{\rho_f}, \frac{\mu_m}{\mu_w}, \frac{1}{\tan(\theta/2)}, \frac{L_c}{D_c}, \cos(i/2) \right) \quad (12)$$

The throughput equation

$$Q = f_Q \left(\frac{D_o}{D_c}, \frac{D_u}{D_c}, P, \frac{V_h}{V_t}, \frac{D_i}{D_c}, \frac{1}{\tan(\theta/2)}, \frac{L_c}{D_c}, \cos(i/2), D_c \right) \quad (13)$$

The relationships were investigated using the EXCEL SOLVER (Multiple linear fitting routine) by minimizing the sum of the squares of error between measured values to the predicted model values. The fitting routine estimates the parameter values in the equations tested. A very large number of equation forms were investigated. Each one was assessed in terms of goodness of fit, fitting statistics, improvement over existing parameters, and practical utility. The final model equations, presented below, are those which were found to be the best according to these criteria. Values of the material-geometry dependent system constants for the model equations are needed to be fitted for the given material and cyclone diameters.

The following relationships were found to be the best for predicting the cut-size, water split, capacity and the sharpness of separation:

The water split, R_f

$$R_f = K_w \left(\frac{D_o}{D_c} \right)^{-1.06787} \left(\frac{D_u}{D_c} \right)^{2.2062} \left(\frac{V_t^2}{R_{\max} g} \right)^{-0.20472} \left(\frac{1}{\tan(\theta/2)} \right)^{0.829} \left(\frac{\mu_m}{\mu_w} \right)^{-0.7118} \left(\frac{L_c}{D_c} \right)^{2.424} \left(\frac{V_h}{V_t} \right)^{-0.8843} \left(\frac{\rho_s - \rho_f}{\rho_f} \right)^{0.523} \left(\cos(i/2) \right)^{1.793} \quad (14)$$

The cut size equation

$$\frac{d_{50c}}{D_c} = K_d \left(\frac{D_o}{D_c} \right)^{1.093} \left(\frac{D_u}{D_c} \right)^{-1.00} \left(\frac{(1-fv)^2}{10^{(1.82*fv)}} \right)^{-0.703} (\text{Re})^{-0.436} \left(\frac{D_i}{D_c} \right)^{-0.936} \left(\frac{L_c}{D_c} \right)^{0.187} \left(\frac{1}{\tan(\theta)} \right)^{-0.1988} \left(\cos\left(\frac{i}{2}\right) \right)^{-1.034} \left(\frac{\rho_s - \rho_f}{\rho_f} \right)^{-0.217} \quad (15)$$

Volume throughput, Q

$$Q = K_{Q0} \left(\frac{D_i}{D_c} \right)^{0.45} D_c^2 \sqrt{P/\rho_p} \left(\frac{D_o}{D_c} \right)^{1.099} \left(\frac{D_u}{D_c} \right)^{0.037} (1/\tan(\theta/2))^{0.405} \left(\frac{L_c}{D_c} \right)^{0.30} \left(\frac{V_h}{V_t} \right)^{-0.048} \left(\cos(i/2) \right)^{-0.092} \quad (16)$$

The Sharpness of separation, α

$$\alpha = K_\alpha \frac{\left(\frac{D_o}{D_c} \right)^{0.27} \left(\frac{V_t^2}{gR_{\max}} \right)^{0.016} \left(\cos\left(\frac{i}{180}\right) \right)^{0.868} \left(\frac{(1-fv)^2}{10^{(1.82*fv)}} \right)^{0.72}}{\left(\frac{D_u}{D_c} \right)^{0.567} \left(\frac{(\rho_s - \rho_p)}{\rho_s} \right)^{1.837} \left(\frac{\mu_m}{\mu_w} \right)^{0.127} \left(1/\tan(\theta/2) \right)^{0.182} \left(\frac{L_c}{D_c} \right)^{0.2}} \quad (17)$$

A comparison of the water split predictions results for the model in equation (14) to those of the Nageswararao model is given in Figure 7. It can be seen that the predicted R_f from the model in equation (14) matches the experimental data better than the predictions from the Nageswararao model. The error with Nageswararao (1978) water split model is about 63%, whereas with the new water split model error is about 30%.

Figure 7: Comparison of new R_f model predictions with Nageswararao (1978) model

The high powers on the relative vortex finder, relative spigot, cone angle, cylindrical length, inclination, and feed solids represented in terms of a hindered settling factor and viscosity in the new water split equation suggests that these have a high influence than the G-forces or the deportment of water in the hydrocyclone. A comparison of the predictions results for cut-size in

equation (15) to those of the Nageswararao model is given in Figure 8. The predicted d_{50c} from the model in equation (15) matches the experimental data well and shows an improvement in the level of accuracy when compared to the Nageswararao model. The new d_{50c} model predictions have a standard error of 19% error whereas the Nageswararao (1978) model predictions have a standard error level of 27.0%. It must be mentioned here that the cut size predictions in the Nageswararao model fairly good particularly in the plus 250 microns range.

Figure 8: Comparison of new d_{50c} model predictions with Nageswararao (1978) model

A comparison of the predictions results from the new volumetric throughput or capacity to those of the Nageswararao model is given in Figure 9. It can be seen that the predicted Q from both model matches the experimental data well and the level of accuracy on the predictions is very similar. The standard error for the Nageswararao capacity equation is about 10.47 %, whereas with the standard error for the new equation is about 9.79 %. The noticeable differences in the capacity equation between the Nageswararao and the new model is the incorporation of the spigot diameter and feed solids effect in terms of hindered settling function in the new equation. The coefficient for the cone angle has also been changed to -0.405. The significance of these additional variables is not as important compared to vortex finder diameter, cone angle, length of cylindrical section and operating pressures, but captures what is observed in practice well.

Figure 9: Comparison of new Q - P model predictions with Nageswararao (1978) Q - P model

The equation for predicting the sharpness of separation is given in equation (17). Equation (17) shows that the sharpness of separation, is a function of slurry properties such as slurry viscosity and density, design variables such as D_o , D_u , D_i , D_c and cone angle, θ , as well as the flowrate, Q_f as G-force factor in a given cyclone.

The slurry viscosity and density are interrelated and their effect on sharpness of separation cannot be easily decoupled Narasimha (2010). However it could be inferred from this equation

that an increase in slurry viscosity and/or density will bring about a decrease in the sharpness of separation value, which is in agreement with the conclusions of other researchers (Asomah 1996, Kojovic 1988).

Nageswararao did not develop an explicit equation for predicting the sharpness of separation. Therefore the authors have compared their predictions with results what is obtained using Asomah's model (1996). The measured versus predicted values for the sharpness of separation equations for new alpha model and Asohma (1996) model are shown in Figure 10.

Figure 10: Comparison of new sharpness of the efficiency curve model predictions with Asomah (1996) model

The standard error for the new sharpness of separation model predictions is 23.4% whereas the Asomah (1996) model predictions is 41.5%.

5. Model validation

224 additional data sets were used to validate the new hydrocyclone model. The data sets which were used to validate the model were not part of the model development data sets. The application-dependent system constants were refitted to each set of data in all cases, but the parameter values in equations 14-17 were not changed. A summary of the model validation data sets on various cyclone sizes is given in Table 2.

Table 2: Summary of supplementary data sets used for model validation.

5.1. Krebs D4, D6 and D10 data sets

These data sets comprise 122 tests conducted in 4, 6 and 10 inch Krebs cyclones using fine limestone material. In all cases, the cyclone was operated vertically. The data is captured whilst the cyclone was operated with 10-50 wt% feed solids, spigot range of 16-28 mm, vortex finder range of 17-78 mm and feed pressure range of 50-200 kpa. These data sets were used to validate the four equations. Figure 11 shows the measured versus model predicted values of the throughput, water recovery to underflow, cut-size and the sharpness of separations for the three

Krebs cyclones tested. The comparison shows that the model predicts d_{50c} , R_f , Q predicts fairly well. The predictions for the sharpness of separation are reasonably good.

Figure 11: Measured versus predicted values for D4 , D6 and D10 Krebs cyclones data sets

5.2. 120 cm cyclone Nageswararo (1978) data

These data sets comprise 22 tests from Nageswararo (1978) data base for large-scale (120 cm) cyclone. As described by Nageswararo (1978), the cyclone was operated at Bougainville copper ore mine using the primary cyclone overflow Copper ore fines as the cyclone feed material. The cyclone was operated with 40-60 wt% (high feed solids) feed solids, spigot range of 200-350 mm, vortex finder of 600 mm and feed pressure range of 30-50 kPa. These data sets are also independent from the model development data sets.

Figure 12 shows the measured versus model predicted values of the throughput, water recovery to underflow and cut-size for the 120 cm large-scale cyclone data. The model predictions were generally good for all three equations.

Figure 12: Measured versus predicted values for 120 cm cyclone (Nageswararo (1978)) data

5.3. JKTech data sets

Nearly 80 data sets of the JKTech were used to validate further the cyclone model equations. These data sets were used for the model validation process. These tests were carried out with 381, 25.4, 15, 10 cm diameter Warman hydrocyclones.

Figure 13 shows the measured versus predicted values of Q , d_{50c} , R_f and α , for the JK TECH data sets. The model predictions were again quite good for Q , d_{50c} and R_f models, whereas α predictions were poorly predicted. Since the original model equations are developed for the cyclones geometrically similar of Krebs design. One should carry extensive design of experiments in Warman cyclones in future in order to build perfect models.

Figure 13: Measured versus predicted values for the JKTech data sets.

6. Model applicability and limitations

The model developed in this study offers a number of advantages including:

- Significant improvement in underflow water split (R_f) predictions in comparison to other models
- Influence of hydrocyclone inclination, feed slurry viscosity and particle density on the hydrocyclone performance are included in the model equations
- An equation for sharpness of the separation is included that allows prediction for changes in particle deportment with improved cyclone operation
- The effect of solids concentration on hydrocyclone performance was accounted for through the viscosity and particle hindered settling rates terms leading to improved model predictions for changes in feed solids concentration.
- An explicit term has been included which accounts for differences in feed slurry viscosity for a range of particle size distributions and solids concentrations. This term takes into account the influence of fine particles on viscosity.

Improved predictions of the performance of hydrocyclones can be made using this new model because in addition to the influence of key design variables terms that account for most of the fluid and particle flow characteristics have been included. The data used to develop the model in this work has a wide range of feed solids concentration from low (3%) to high (70%) solids by weight.. This new model is also implemented into JKSimMet 6.0 version as a potential model for industrial classification predictions.

Although the new model predicts the performance of hydrocyclones reasonably well it has a number of limitations/requirements that should be taken into account when using this model;

- Model parameters need to be fitted at least to one set of experimental data for a given feed material and design conditions.

- Although the model can be applied to sub 10 microns feed materials the model has not been tested sufficiently for applications in this size range and the response has not been verified.
- This model is unaccounted the fish-hook phenomena
- The prediction of sharpness of the separation still requires further work due to some scatter observed in the results.
- Though this average particle density based model equations have potential for application to minerals with different density components in the feed further work is required to improve predictions for such feed materials.

7. Conclusions

An improved Empirical hydrocyclone model was developed from a data base comprising historical data from hydrocyclone tests performed by numerous researchers and additional tests were performed by the authors to capture variables that were not included in the historical data base. Inputs on particle classification mechanism from CFD were considered to understand and identify the key flow parameters that affect the cyclone performance in the application involving particle classification by size. The new cyclone model structure is based on the dimensionless approach makes it possible to combine geometry dimensions and as well as flow terms in simple equations that can be used to predict performance measured by efficiency curve properties and capacity. The following conclusions can be made from the new cyclone model developed in this work:

- An extensive data base covering a wide range of cyclones is collocated from historical experimental data sets and additional experiments. Experiments on 10 and 20 inch Krebs cyclones were performed to fill the gaps in the data base, especially at low to moderate feed solids concentration and at different cone sections.
- Inputs from CFD studies were considered in understanding the flow pattern of fluid and solid particles inside cyclones. Tangential velocity, turbulent diffusion, slurry viscosity and particle hindered settling correlations were identified from CFD as the key inputs to the particle classification mechanism for the Empirical model.

- A new cyclone model structure based on a dimensionless approach has been developed. The approach used to develop the model is based on multiple linear fitting routine for model parameters estimation.
- The model for R_f , d_{50c} , Q give a very good fit to the data compare to Nageswararao (1978) models. While the model for the separation sharpness gave reasonable correlations with the cyclone design and operating conditions. Compared to Asomah (1996)'s separation sharpness model, the new model predicts an improved values.
- 224 additional data sets were used to validate the new hydrocyclone model by comparing the predictions of the model equations with the experimental results. The data sets which were used to validate the model were not part of the model development data sets. The application-dependent system constants (K_w , K_d , K_Q , K_a) were refitted to each set of data in all cases.

8. Acknowledgments

The authors would like to express their sincere thanks to Prof. Emmy Manlapig, Manager, AMIRA P9N, JKMRRC, University of Queensland, Australia, and AMIRA-P9N & P9O research sponsors and management, for their keen interest, encouragement and funding for undertaking these studies.

9. Nomenclature

θ	Cone angle of cyclone (degree)
d_{50c}	corrected separation (classification) size
D_c	cyclone diameter
D_i	inlet diameter
D_o	vortex finder diameter
D_u	spigot diameter
Ea	actual efficiency
Ec	corrected efficiency

Eu Euler number = $\frac{Dp}{1/2 \cdot r \cdot v^2}$ = pressure loss factor based on the static pressure

drop across the cyclone

f_s feed percent solids in cyclone feed slurry (wt.)

f_v feed volume fraction of solids

$F_{-38\mu}$ Fine fraction below 38 μ m in the cyclone feed

g acceleration due to gravity

h free vortex height of cyclone (distance from bottom of vortex finder to the top of spigot)

i inclination angle, degrees

L_c cylinder length

L cyclone length

$P, \Delta p$ cyclone inlet pressure, pressure drop across the cyclone

P_{40} size 40% feed material passing

P_{80} size 80% feed material passing

Q, Q_F feed volume flow rate

R radius of cyclone

R_a radius of air core at the discharge level

R_C Cyclone radius, m

Re Reynolds number = $\frac{v \cdot D_c \cdot r}{m}$;

where v inlet velocity = $\frac{4Q}{\pi D_c^2}$

R_f fraction of feed water to underflow

R_v	volumetric recovery of feed to underflow
v	characteristic fluid velocity in a cyclone (subscripts: t = tangential, r = radial, z = axial)
V_C	Cyclone periphery tangential velocity, m/s
V_h	particle hindered settling velocity, m/s
V_t	particle terminal settling velocity, m/s
α	sharpness of separation or cut
α_{loss}	velocity reduction factor
μ	fluid viscosity (subscripts: p = pulp or m = slurry, l = liquid, w = water)
ρ	fluid density (subscripts: p = pulp or m = slurry or suspension, l = liquid, s = solid)
ϕ	feed volume % solids

10. References

- Asomah, A.K., 1996. Improved models of hydrocyclones. PhD thesis, The University of Queensland..
- Boysan, F., Ayers, W.H., Swithenbank, J., 1982. A fundamental mathematical modelling approach to cyclone design. *Trans. Instn Chem Engrs* 60, 222-230.
- Bradley, D., 1965. *The Hydrocyclone*. Pergamon Press Ltd, London
- Brennan, M.S., Narasimha, M., Holtham, P.N., 2007. Multiphase modelling of hydrocyclones - prediction of cut-size. *Minerals Engineering* 20, 395-406.
- Castro, O., 1990. An investigation of pulp rheology effects and their application to the dimensionless type hydrocyclone models. M.Eng.Sc. Thesis, University of Queensland.
- Delgadillo, J.A., Rajamani, R.K., 2005. A comparative study of three turbulence-closure models for the hydrocyclone problem. *International Journal of Mineral Processing* 77, 217-230.

- Griffiths, W.D., Boysan, F., 1996. Computational fluid dynamics and empirical modelling of a number of cyclone samplers. *Journal of Aerosol Science* 27, 281-304.
- He, P., Salcudean, M., Gartshore, I.S., 1999. A numerical simulation of hydrocyclones. *Chemical Engineering Research and Design* 77, 429-441.
- He, Y.B., Laskowski, J.S., 1994. Effect of dense medium properties on the separation performance of a dense medium cyclone. *Minerals Engineering* 7, 209-221.
- Hinde, A.L., Jennery, G.R., Mackay, J.G., 1979. The classification performance of a hydrocyclone. Chamber of Mines of South Africa Research Organisation, pp. 1-61.
- Hsieh, K.T., Rajamani, K., 1988. Phenomenological model of the hydrocyclone: Model development and verification for single-phase flow. *International Journal of Mineral Processing* 22, 223-237.
- Hsieh, K.T., Rajamani, K., 1991. Mathematical model of the hydrocyclone based on physics of fluid flow. *AIChE Journal* 37, 735-746.
- Ishii, M., Mishima, K., 1984. Two-fluid model and hydrodynamic constitutive relations. *Nuclear Engineering and Design* 82, 107-126.
- Kojovic, T., 1988. The development and application of MODEL - An automated model builder for mineral processing. PhD thesis, The University of Queensland.
- Lilge, E.O., 1962. Hydrocyclone fundamentals. *IMM Trans (Bulletin)*, 523-546.
- Lynch, A.J., 1977. *Mineral Crushing and Grinding Circuits: Their Simulation, Optimisation, Design and Control*. Elsevier Scientific Publishing Company 340, 340.
- Lynch, A.J., Rao, T.C., 1968. Studies on the operating characteristics of hydrocyclone classifiers. *Indian Journal of Technology* 6, 106-114.
- Lynch, A.J., Rao, T.C., 1975. Modelling and scale up of hydrocyclone classifiers (also discussion of paper), XI IMPC, Cagliari, pp. 9-25.
- Lynch, A.J., Rao, T.C., Bailey, C.W., 1975. The influence of design and operating variables on the capacities of hydrocyclone classifiers. *IJMP* 2, 29-37.
- Mackay, J.G., Hinde, A.L., Loclier, A., Wilson, A., 1981. Hydrocyclone performance at high cut sizes. Chamber of Mines of South Africa, pp. 1-71.
- Mainza, A., N., Olson, T., Powell, M.S., Stewart, T., 2006. P9N Private communication.
- Mainza, A.N., 2006. Contributions to the Understanding of Three Product Cyclones in the Classification of Dual Density Platinum Ores. PhD Thesis, The University of Cape Town.

- Mangadoddy Narasimha, Brennan, M.S., Holtham, P.N., Banerjee, P.K., 2007. Numerical analysis of the changes in dense medium feed solids on dense medium cyclone performance., 16th Australasian Fluid Mechanics Conference (AFMC), Gold Coast, Queensland, Australia, pp. 1042-1049.
- Mangesana, N., Mainza, A. A., Govender, I., van der Westhuizen, A. P., Narasimha, M., 2008. The effect of particle sizes and solids concentration on the rheology of silica sand based suspensions. *Journal of the South African Institute of Mining and Metallurgy* 108, 237-243.
- Marlow, D., 1973. A mathematical analysis of hydrocyclone data. M.Sc. thesis, University of Queensland.
- Nageswararao, K., 1978. Further developments in the modelling and scale-up of industrial hydrocyclones. PhD thesis, The University of Queensland.
- Narasimha, M., 2010. Improved computational and empirical models of hydrocyclones. University of Queensland, JKMRRC.
- Narasimha, M., Brennan, M., Holtham, P.N., 2006a. Large eddy simulation of hydrocyclone-prediction of air-core diameter and shape. *International Journal of Mineral Processing* 80, 1-14.
- Narasimha, M., Brennan, M., Mainza, A.N., Holtham, P.N., 2010. Towards improved hydrocyclone models: Contributions from CFD, (IMPC 2010), , 6-10th Sep, 2010., XXV International Mineral Processing Congress.
- Narasimha, M., Brennan, M.S., Holtham, P.N., Napier-Munn, T.J., 2006b. A comprehensive CFD model of dense medium cyclone performance. *Minerals Engineering* 20, 414-426.
- Narasimha, M., Brennan, M.S., Holtham, P.N., Napier-Munn, T.J., 2007. A comprehensive CFD model of dense medium cyclone performance. *Minerals Engineering* 20, 414-426.
- Narasimha, M., Brennan, M. S., Holtham, P. N. and Banerjee, P. K. , 2007. Numerical Analysis of the Changes in Dense Medium Feed Solids on Dense Medium Cyclone Performance. In: Jacobs, Peter, McIntyre, Tim, Cleary, Matthew, Buttsworth, David, Mee, David, Clements, Rose, Morgan, Richard and Lemckert, Charles, 16th Australasian Fluid Mechanics Conference (AFMC). Gold Coast, Queensland, Australia, 1042-1049.
- Narasimha, M., Sripriya, R., Banerjee, P.K., 2005. CFD modelling of hydrocyclone-prediction of cut size. *International Journal of Mineral Processing* 75, 53-68.
- Neesse, T., 1971. The hydrocyclone as a turbulence classifier. *Chemie Technik* 23, 146-152.

- Neesse, T., Dallman, W., Espig, D., 1986. Effect of turbulence on the efficiency of separation in hydrocyclones at high feed solids concentrations. *Aufbereitungs Technik* 919, 6-14.
- Nowakowski, A.F., Cullivan, J.C., Williams, R.A., Dyakowski, T., 2004. Application of CFD to modelling of the flow in hydrocyclones. Is this a realizable option or still a research challenge? *Minerals Engineering* 17, 661-669.
- Nowakowski, A.F., Kraipech, W., Williams, R.A., Dyakowski, T., 2000. Hydrodynamics of a hydrocyclone based on a three-dimensional multi-continuum model. *Chemical engineering journal* 80, 275-282.
- Plitt, I.R., 1976. A mathematical model of the hydrocyclone classifier. *CIM Bulletin* December, 114-122.
- Rao, T.C., 1966. The characteristics of hydrocyclones and their application as control units in comminution circuits. PhD thesis, The University of Queensland.
- Richardson, J.F., Zaki, W.N., 1954. Sedimentation and fluidisation. Part 1. *trans. Inst. Chem. Eng.* 32, 35-53.
- Shi, F., 1994. Slurry rheology and its effects on grinding. University of Qld.
- Steinour, H.H., 1944. Rate of sedimentation, suspensions of uniform size angular particles. *Industrial and Engineering Chemistry* 36, 840-847.
- Suasnabar, D.J., 2000. Dense medium cyclone performance, enhancements via computational modeling of the physical process. Ph.D. Thesis, University of New South Wales, Sydney.
- Svarovsky, L., 1984. *Hydrocyclones*.
- Tavares, L.M., Souza, L.L.G., Lima, J.R.B., Possa, M.V., 2002. Modeling classification in small diameter hydrocyclones under variable rheological conditions. *Minerals Engineering* 15, 613-622.
- Xiao, J., 1997. Extensions of model building techniques and their applications in mineral processing. Ph.D. Thesis, The University of Queensland.

List of the Figures:

Figure 1: Cyclone efficiency curves for Krebs 20 inch design

Figure 2: Comparison of tangential velocity profiles with $n=0.71$ in D6 cyclone

Figure 3: Comparison of tangential velocity profiles with (a) $n=0.76$ in D10 cyclone and (b) $n=0.77$ in D15 cyclone

Fig 4: Rheograms of magnetite slurry (He and Laskowski, 1994)

Fig 5: Rheograms of silica slurry (Magesena et al 2008)

Fig 6: Comparison of predicted slurry viscosity by Ishii and Mishima (1984) and new model with the measured values

Fig 7: Comparison of new R_f model predictions with Nageswararao (1978) model

Fig 8: Comparison of new d_{50c} model predictions with Nageswararao (1978) model

Figure 9: Comparison of new Q-P model predictions with Nageswararao (1978) Q-P model

Fig 10: Comparison of new α model predictions with Asomah (1996) model

Fig 11: Measured versus predicted values for D4 , D6 and D10 Krebs cyclones data sets

Figure 12: Measured versus predicted values for 120 cm cyclone (Nageswararao (1978)) data

Figure 13: Measured versus predicted values for the JKTech data sets.

List of the Tables:

Table 1: Data collection

Table 2: Standard deviations of the efficiency curve fitting parameters for Mainza et al [25] series

Table 3: Summary of supplementary data sets used for model validation

ACCEPTED MANUSCRIPT

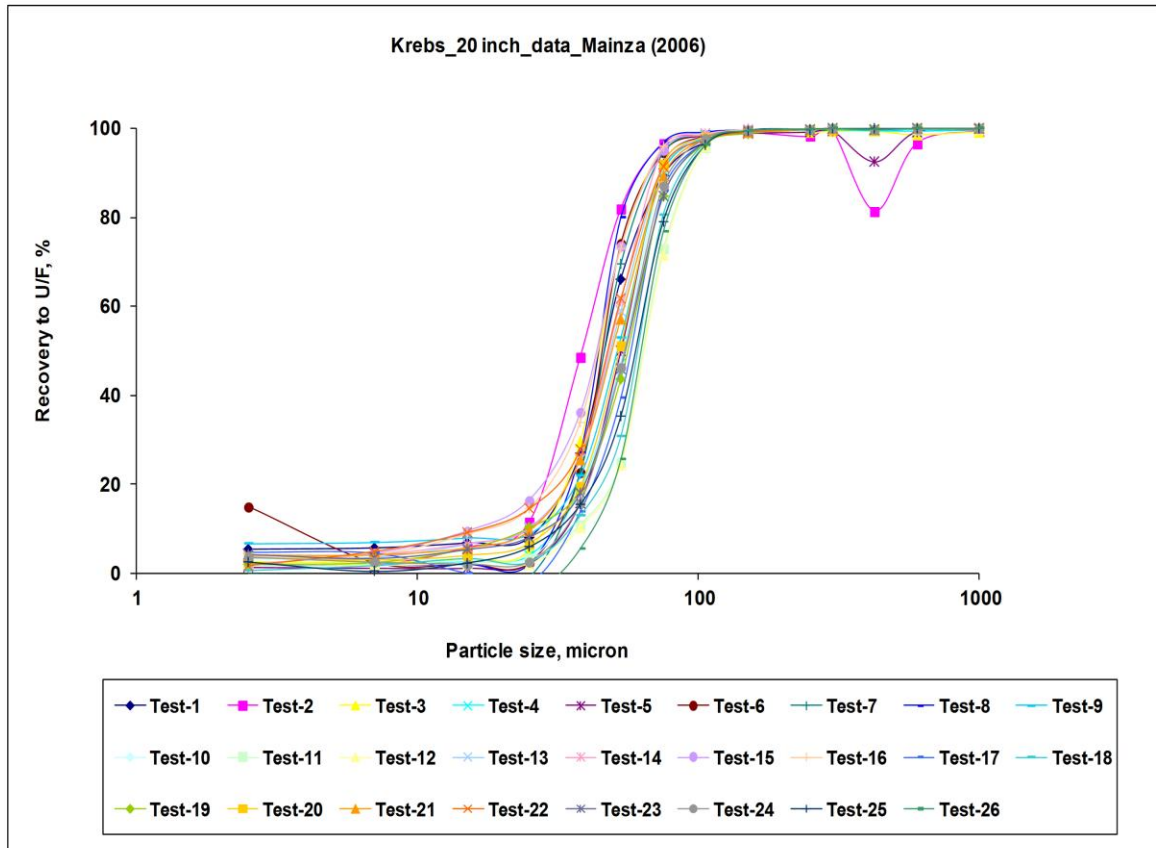


Figure 1

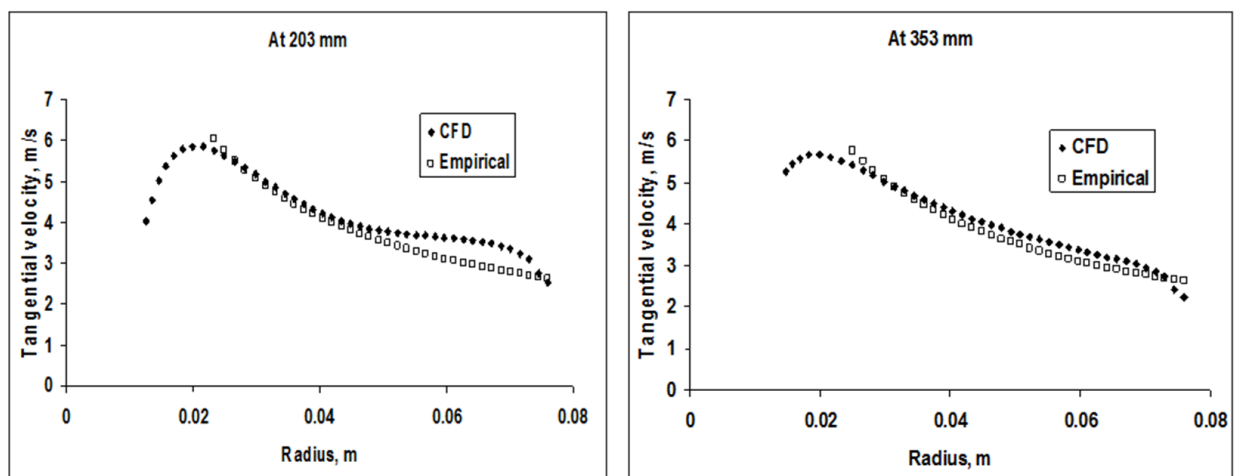


Figure 2

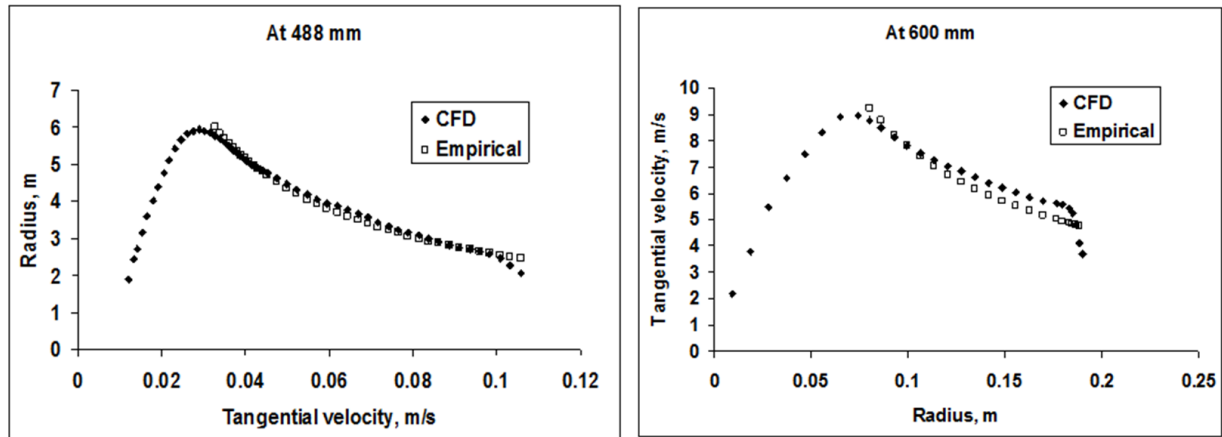


Figure 3

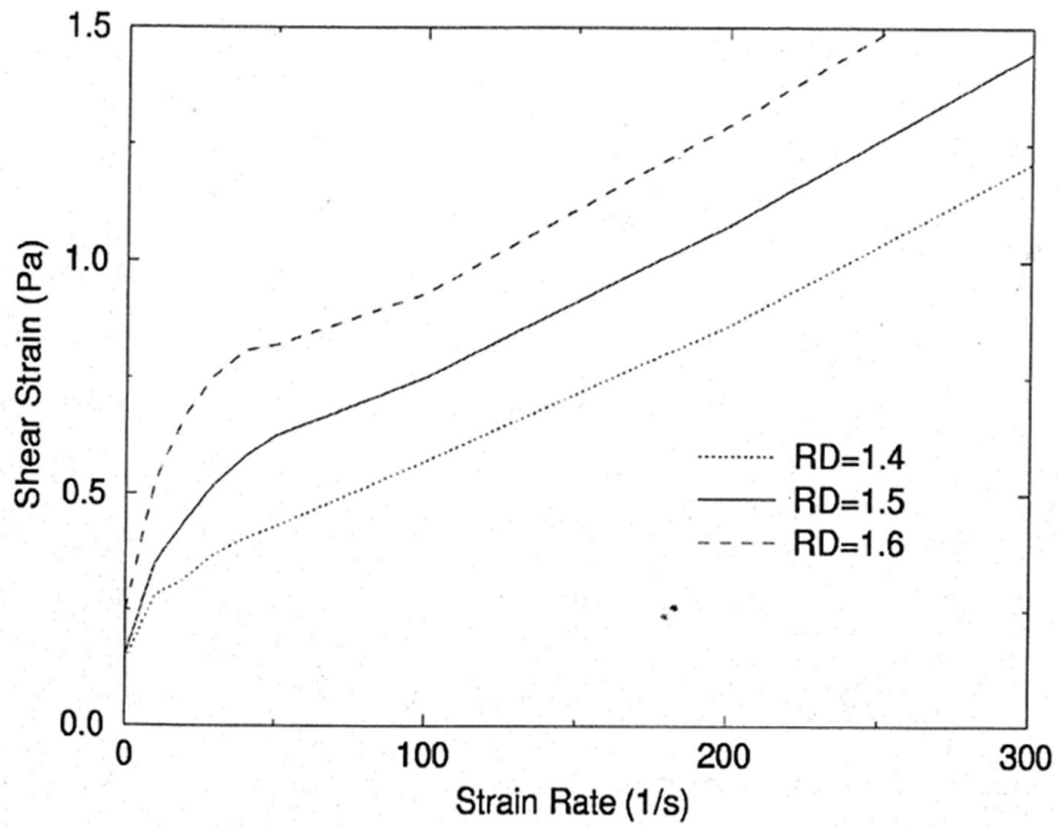


Figure 4

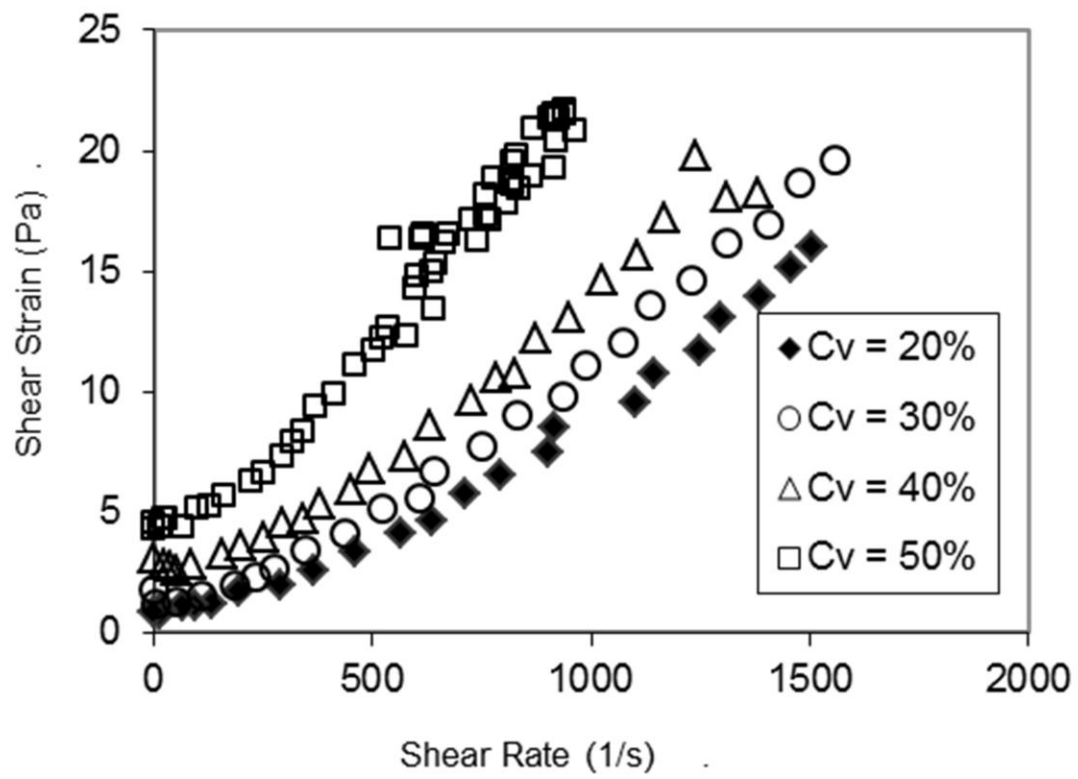


Figure 5

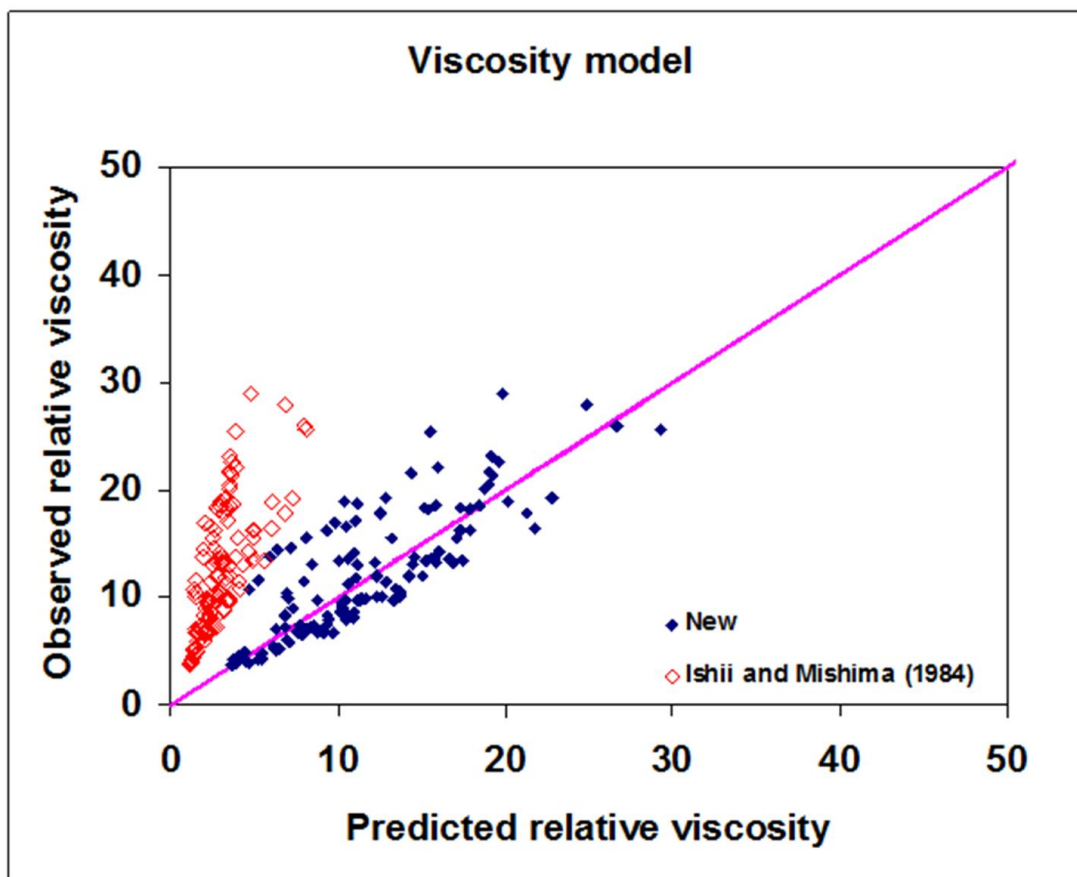


Figure 6

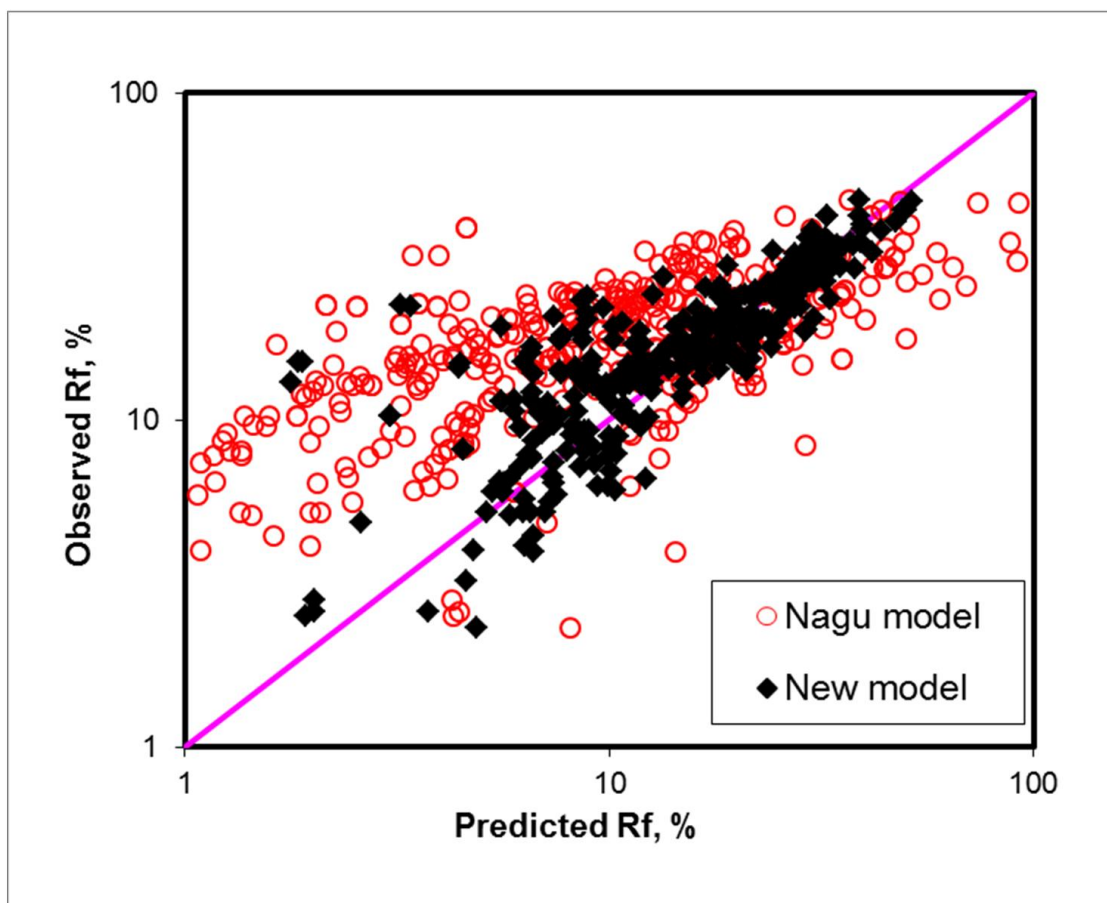


Figure 7

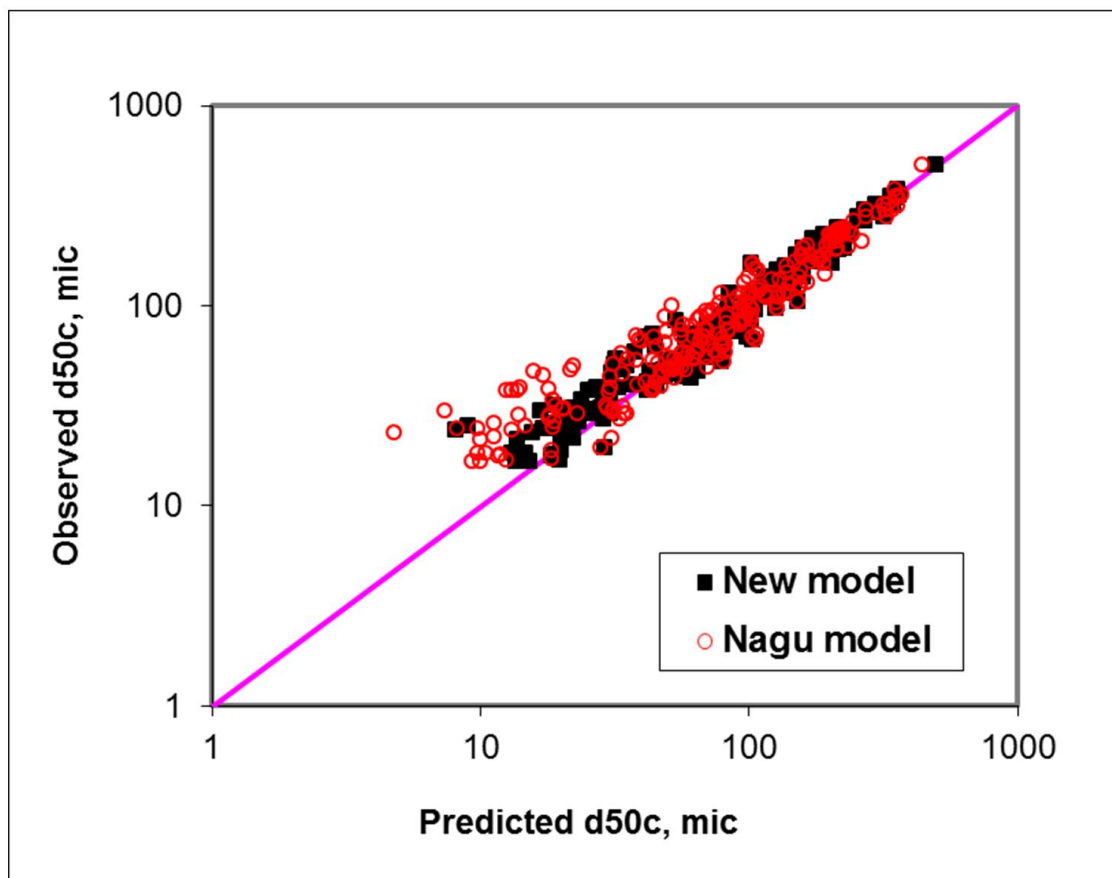


Figure 8

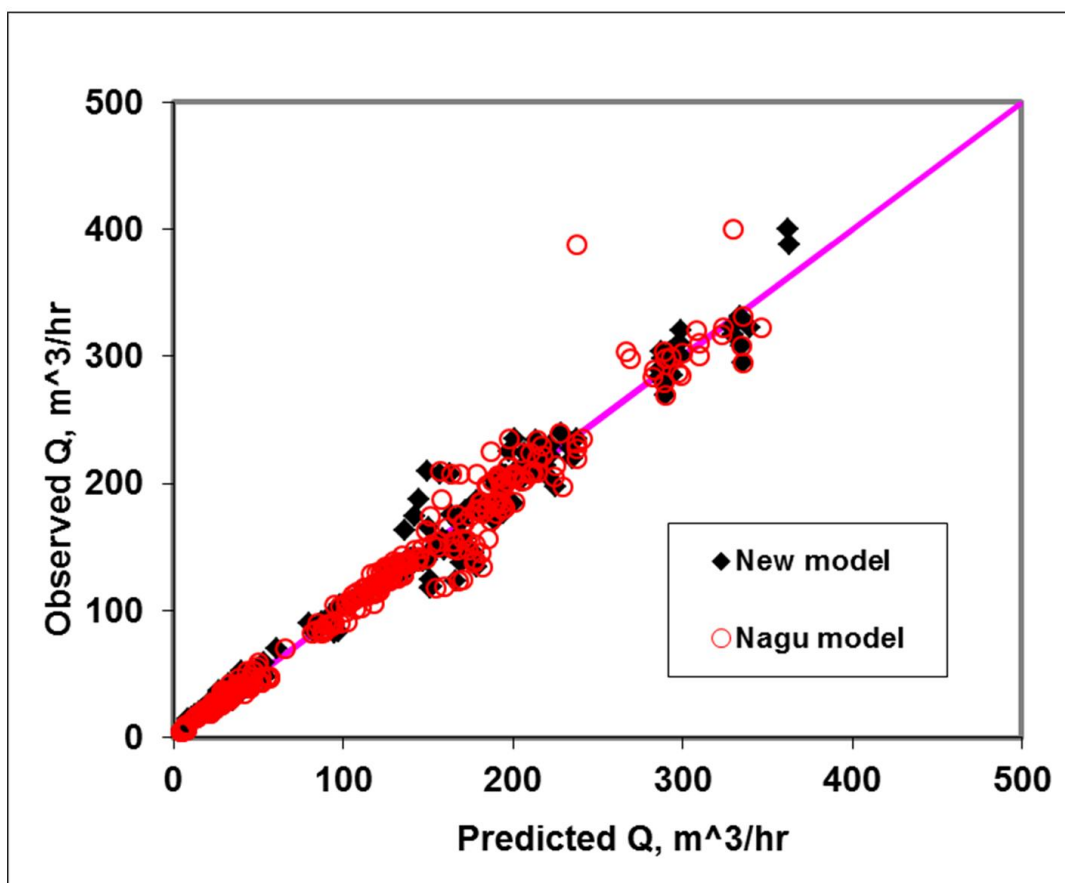


Figure 9

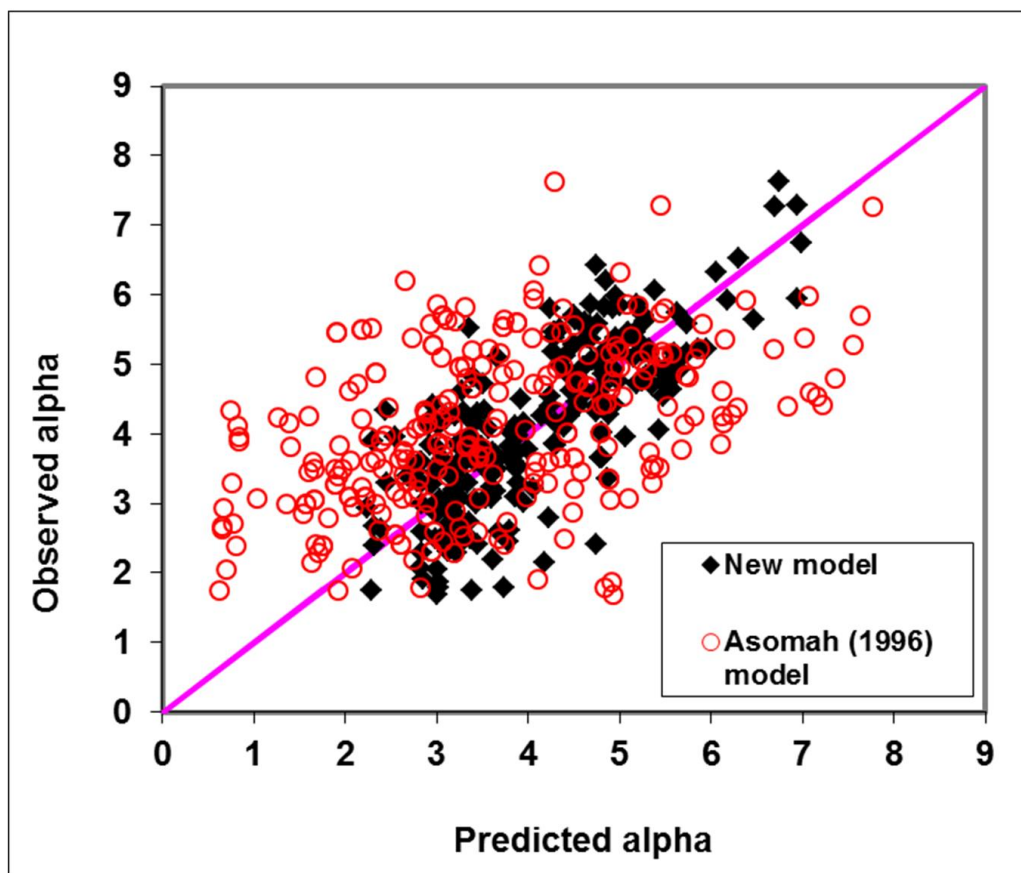


Figure 10

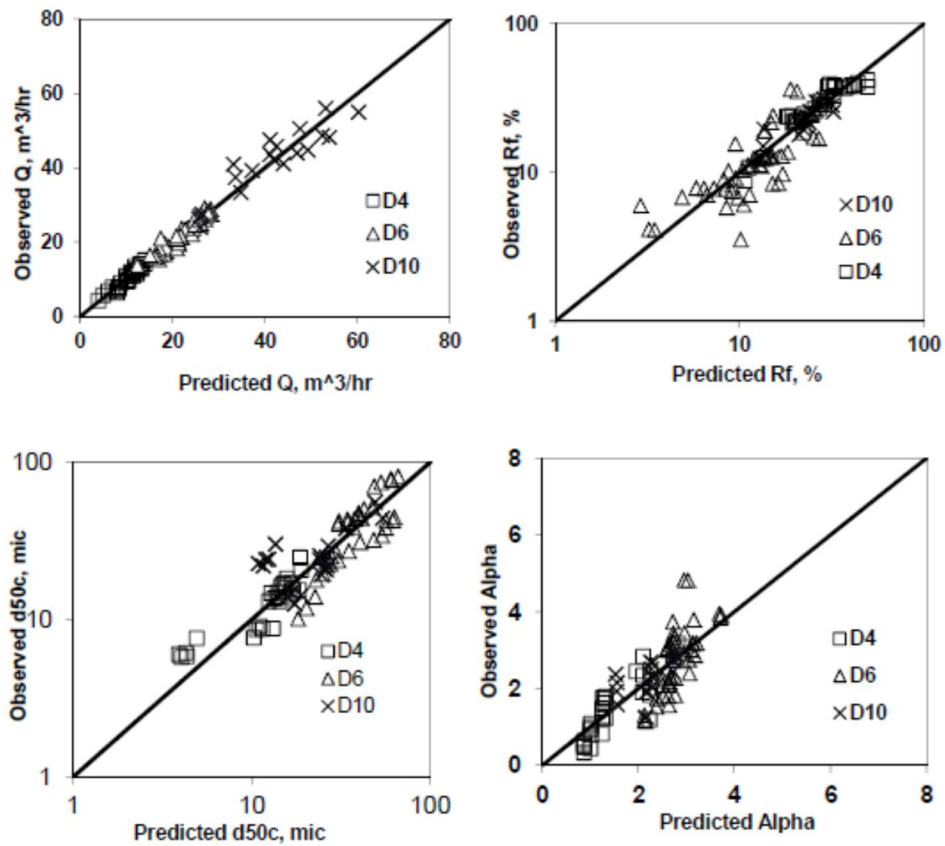


Figure 11

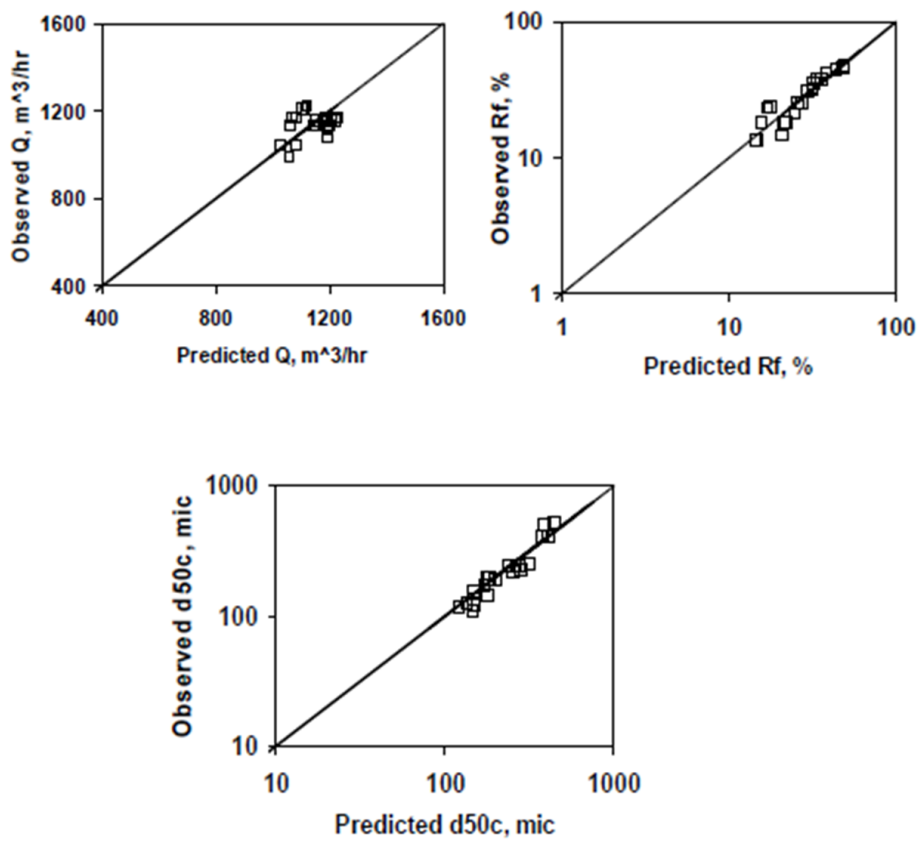


Figure 12

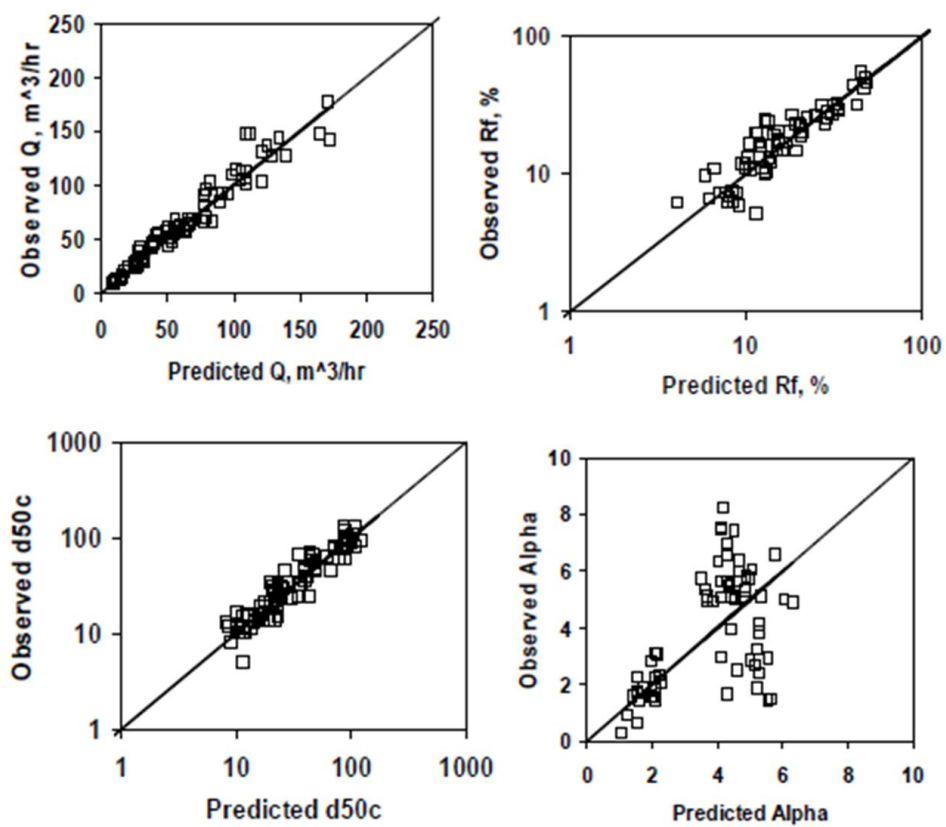


Figure 13

Table 1: Data collection

Data Source	Diameter of cyclone (inches)	No. of tests	Material	Aim of the tests
Rao [1]	20	91	Silica	Design variables effect
	6	25	Silica	Design variables effect
Nageswararao [5]	15	14	Limestone	Design variables effect
	10	11	Limestone	Design variables effect
	6	20	Limestone	Cone angle & cyclone length effects
	4	3	Limestone	Design variables effect
Castro [8]	10	30	Limestone	Viscosity effect
	20	26	Mt Isa-Copper ore	Viscosity effect
Asomah [10]	4	21	Mt Leyson	Inclination effect (0-135 degrees)
	4	17	Limestone	Inclination effect (0-67.5 degrees)
	20	10	Pb-Zn ores	Inclination effect (0-90 degrees)
	20	32	Cu-ore	Inclination effect (0-135 degrees)
	20	26	MnO ₂ and Magnetite	Inclination effect (0-90 degrees)
	4	17	Mineral identity tests	Density effect
Mainza et al. ([25])	20	23	Tailings	Low percent feed solids effect
Narasimha [26]	10	25	Limestone	Cone angle-low feed solids effect
Hinde[27]	30	61	Gold minerals	Design variables effect (Tangential inlet)
Castro [8]	30	27	Limestone	Spigot and feed solids effects
Total data sets		479		

Table 2: Standard deviations of the efficiency curve fitting parameters for Mainza et al [25] series

Test No.	Stdev	Remark	Test No.	Stdev	Remark
T1	2.706805		T14	1.72577	
T2	5.093553	Rejected	T15	1.623081	
T3	1.452174		T16	1.811158	
T4	1.099117		T17	2.487352	
T5	4.294604	Rejected	T18	1.305326	
T6	4.334167	Rejected	T19	1.53409	
T7	1.601805		T20	1.382568	
T8	1.210095		T21	1.451335	
T9	2.645263		T22	1.878071	
T10	1.512631		T23	1.549191	
T11	1.209600		T24	1.371612	
T12	1.131119		T25	1.017412	
T13	1.388801		T26	2.617663	
Avg. Stdev			1.978245		

Table 3: Summary of supplementary data sets used for model validation

Data Source	Diameter of cyclone (inches)	No. of tests	Material	Aim of the tests
Narasimha [26]	4	36	Limestone	feed solids effect Design & operating variables
	10	30	Limestone	Cone angle-low feed solids effect
	6	56	Limestone	feed solids effect Design & operating variables
Nageswararao [5]	50	22	Copper ore	Feed solids effect Pressure & spigot variations
JK TECH data	4, 5, 10 & 20	80	Various mineral slurries	Operating & Design variables effect

Highlights

- A semi-mechanistic hydrocyclone model is developed based on dimensionless approach
- The inputs from CFD simulations and industrial cyclone performance data are used
- The model for R_f , d_{50c} , Q gives a very good fit to the experimental data.
- The α model gives reasonable correlation with the cyclone experimental data
- New semi-empirical cyclone model is validated extensively with additional data sets